Author Manuscript

Author Manuscript

Author Manuscript

Author Manuscript

HHS Public Access

Author manuscript

Hippocampus. Author manuscript; available in PMC 2019 July 29.

Published in final edited form as:

Hippocampus. 2016 January ; 26(1): 110–117. doi:10.1002/hipo.22495.

17β Estradiol Recruits GluN2B-containing NMDARs and ERK During Induction of Long-Term Potentiation at Temporoammonic-CA1 Synapses

Caroline C Smith[1], **Lindsey A Smith**[2], **Teruko Bredemann**[2], **Lori L. McMahon**[1,2,3]

[1]Departments of Physiology and Biophysics, University of Alabama at Birmingham, Birmingham, AL 35294-0005

[2]Departments of Cell, Developmental, and Integrative Biology, University of Alabama at Birmingham, Birmingham, AL 35294-0005

[3]Evelyn F. McKnight Brain Institute, University of Alabama at Birmingham, Birmingham, AL 35294-0005

Abstract

When circulating 17β estradiol (E2) is elevated to proestrous levels, hippocampus-dependent learning and memory is enhanced in female rodents, non-human primates, and women due to heightened synaptic function at hippocampal synapses. We previously reported that proestrous-like levels of E2 administered to young adult ovariectomized female rats increases the magnitude of LTP at CA3 Schaffer collateral (SC)-CA1 synapses only when dendritic spine density, the NMDAR/AMPAR ratio, and current mediated by GluN2B-containing NMDA receptors (NMDARs) are simultaneously increased. We also reported that this increase in GluN2B-mediated NMDAR current in area CA1 is causally related to the E2-induced increase in novel object recognition, tying together heightened synaptic function with improved learning and memory. In addition to SC inputs, innervation from the entorhinal cortex in the temporoammonic (TA) pathway onto CA1 distal dendrites in stratum lacunosum-moleculare is critical for spatial memory formation and retrieval. It is not known whether E2 modulates TA-CA1 synapses similarly to SC-CA1 synapses. Here, we report that 24 hours post-E2 injection, dendritic spine density on CA1 pyramidal cell distal dendrites and current mediated by GluN2B-containing NMDARs at TA-CA1 synapses is increased, similarly to our previous findings at SC-CA1 synapses. However, in contrast to SC-CA1 synapses, AMPAR transmission at TA-CA1 synapses is significantly increased, and there is no effect on the LTP magnitude. Pharmacological blockade of GluN2B-containing

Corresponding author with complete address, including an email address: Lori L. McMahon, PhD, Departments of Physiology and Biophysics and Cell, Developmental, and Integrative Biology, Evelyn F. McKnight Brain Institute, University of Alabama at Birmingham, 1918 University Blvd., MCLM 988, Birmingham AL 35294-0005, mcmahon@uab.edu, 205-934-3523.

Authors Addresses:

Caroline C Smith, PhD, Department of Physiology and Biophysics, University of Alabama at Birmingham, 1918 University Blvd., MCLM 960, Birmingham AL 35294-0005, 205-934-3523

Caroline Hamilton PhD, Life Sciences Office, NSCE-2122A, Tarrant County College N.E. Campus, 828 W. Harwood Road, Hurst, Texas 76054, 817-515-6836, Caroline.Hamilton@tccd.edu

Lindsey A Smith, BS, Department of Cell, Developmental, and Integrative Biology, University of Alabama at Birmingham, 1918 University Blvd., MCLM 960, Birmingham AL 35294-0005, smithla@uab.edu

Teruko Bredemann, PhD, Department of Cell, Developmental, and Integrative Biology, University of Alabama at Birmingham, 1918 University Blvd., MCLM 960, Birmingham AL 35294-0005, tmbredem@uab.edu

Author Manuscript Author Manuscript Author Manuscript Author Manuscript

NMDARs or ERK activation, which occurs downstream of synaptic but not extrasynaptic GluN2B-containing NMDARs, attenuates the LTP magnitude only in slices from E2-treated rats. These data show that E2 recruits a causal role for GluN2B-containing NMDARs and ERK signaling in the induction of LTP, cellular mechanisms not required for LTP induction at TA-CA1 synapses in vehicle-treated ovariectomized female rats.

Keywords

Estrogen; hippocampus; NMDA receptors; females; spine density

Introduction

E2 replacement reverses deficits in working, verbal, and spatial memory in naturally and surgically menopausal women (Henderson, 2009; Phillips and Sherwin, 1992; Rocca et al., 2011; Zec and Trivedi, 2002), and improves many forms of hippocampus-dependent learning and memory in female mice, rats, and non-human primates (Frick et al., 2002; Gibbs, 1999; Gresack and Frick, 2006; Rapp et al., 2003; Vedder et al., 2013). In defining the mechanisms contributing to the E2-enhanced learning and memory, much focus has been placed on functional and morphological changes occurring at CA3 Schaffer collateral (SC)-CA1 synapses. At proestrus in ovary intact female rats, or in ovariectomized (OVX) rats treated with exogenous E2 at proestrous-like levels, CA1 pyramidal cell dendritic spine density, current mediated by GluN2B-containing NMDARs, the NMDAR:AMPAR ratio, and the magnitude of LTP at SC-CA1 synapses are increased (Cordoba Montoya and Carrer, 1997; Gould et al., 1990; Smith and McMahon, 2005; Smith and McMahon, 2006; Snyder et al., 2011; Warren et al., 1995; Woolley et al., 1990; Woolley and McEwen, 1994). The increase in current carried by GluN2B-containing NMDARs, likely due to increased synaptically located NMDARs and GluN2B subunit phosphorylation (Vedder et al., 2013), is completely responsible for the heightened LTP magnitude (Smith and McMahon, 2006). Recently, we reported that the E2-induced increase in novel object recognition (NOR) only occurs at time points when the GluN2B-containing NMDAR current and LTP are also increased (Vedder et al., 2013). Furthermore, pharmacological blockade of GluN2B-containing NMDARs in area CA1 via stereotaxically placed cannulas only prevents the E2-enhanced NOR in OVX rats, linking together heightened LTP magnitude (Smith and McMahon, 2006) with heightened NOR (Vedder et al., 2013).

In addition to the input from CA3 pyramidal cells, CA1 pyramidal cells receive a direct cortical input from layer III of the entorhinal cortex (temporoammonic pathway, TA) which synapses onto CA1 distal dendrites in stratum lacunosum-moleculare (SLM). A role for the TA pathway in modifying spatial learning and novelty detection have been established by various lesion (Ferbinteanu et al., 1999; Kirkby and Higgins, 1998; Remondes and Schuman, 2004; Vnek et al., 1995) and pharmacological studies (Hunsaker et al., 2007; Vago et al., 2007; Vago and Kesner, 2008). Experimental data and computer modeling suggest that strong input to CA1 cells from the TA pathway is critical in memory encoding, while strong input from CA3 pyramidal cells is critical during memory retrieval (Manns et al., 2007). These data indicate that activity at both pathways is required for normal

Author Manuscript Author Manuscript Author Manuscript Author Manuscript

hippocampus-dependent learning and memory. Given its position in the circuit and the particular timing of activity, the TA pathway can dictate whether SC-CA1 synapses will drive CA1 pyramidal cells to spike. Additionally, TA-CA1 synapses undergo NMDAR-dependent LTP and LTD (Aksoy-Aksel and Manahan-Vaughan, 2015; Dvorak-Carbone and Schuman, 1999; Remondes and Schuman, 2002), and as such, can either enhance or prevent plasticity at CA3-CA1 synapses (Remondes and Schuman, 2002). It is currently unknown if TA-CA1 synapses are modulated by E2. Given the vital role the entorhinal cortex plays in hippocampus-dependent memory, we asked whether E2 similarly modulates TA-CA1 synapses as a substrate for the enhanced learning.

In this study, we find that E2 replacement at proestrous-like levels in adult OVX rats increases spine density and current mediated by GluN2B-containing NMDARs at TA-CA1 synapses measured at 24 hours post-injection. In contrast to SC-CA1 synapses (Smith and McMahon, 2005), AMPAR transmission is also increased at this time point, while the magnitude of LTP is unchanged. Importantly, although the magnitude of LTP is unaffected by E2, the induction mechanism now requires activation of synaptically located GluN2B-containing NMDARs which are specifically coupled to the ERK signaling cascade (Krapivinsky et al., 2003; Mulholland et al., 2008). Therefore, our data show a causal role for synaptic GluN2B-containing NMDARs and ERK activation in LTP induction at TA synapses following an increase in circulating E2 to proestrous levels. These findings suggest a likely participation of these synapses in the E2-induced enhanced NOR, which we reported also requires GluN2B-containing NMDARs located in area CA1 (Vedder et al., 2013).

Materials and Methods

Animal Treatment

All experimental protocols were performed with permission from the Institutional Animal Care and Use Committee and follow guidelines set forth by the National Institutes of Health.

Surgical procedures were as previously described (Smith and McMahon, 2005). 7–9 week old female Sprague Dawley rats (approx 250g) were bilaterally ovariectomized (OVX). Animals received 2 estradiol (E2) injections (10μg/250g; 24 hr interval) or cotton seed oil subcutaneously 10–20 days following OVX to elicit proestrous-like circulating levels of E2 (Woolley and McEwen, 1993). Experiments were performed 24h following the 2nd estradiol (E24) or oil injections. No significant difference was observed in slices from non-treated and vehicle-treated OVX rats, thus, data were pooled (vehicle, V). Dry uterine weights were obtained to confirm success of OVX and E2 responsiveness (Hall et al., 1992; Smith and McMahon, 2005)(uterine weights: E24; 0.21 ± 0.01g; V; 0.08 ± 0.01g).

Hippocampal Slice Preparation

Rats were anesthetized using 2.5% isoflurane and rapidly decapitated. Brains were removed and coronal slices (400μm for extracellular recordings; 250μm for whole-cell recordings) were prepared from dorsal hippocampus in high sucrose/low Na^+ artificial cerebral spinal fluid (aCSF): [in mM: 85 NaCl2.5 KCl, 4 $MgSO_4$, 0.5 $CaCl_2$, 1.25 NaH_2PO_4, 25 $NaHCO_3$, 25 glucose, 75 sucrose and 0.5 ascorbate (saturated in 95% O_2 and 5% CO_2, pH 7.4)]. Slices

Author Manuscript Author Manuscript Author Manuscript Author Manuscript

were stored in standard aCSF (in mM): 119 NaCl, 26 $NaHCO_3$, 1.5 KCl, 1 NaH_2PO_4, 2.5 $CaCl_2$, 1.3 $MgSO_4$, 26 $NaHCO_3$, and 10 glucose (saturated in 95% O_2 and 5% CO_2, pH 7.4). Slices were held in standard aCSF for 1h in a submersion chamber prior to experimentation where they remained for up to 4h (bubbled with 95% O_2 and 5% CO_2).

Electrophysiology

All experiments were performed in a submersion chamber continuously perfused with aCSF at 2–3ml/min bubbled with 95% O_2 and 5% CO_2 at 26–28ºC. The CA3 region was removed from all slices.

Extracellular Recording.

A recording electrode filled with aCSF was placed within 200μm of the stimulating electrode in stratum lacunosum-moleculare (SLM) of area CA1. LTP experiments were performed by first collecting a 20 min baseline (0.1Hz, 100μs duration) at a stimulus intensity that generated field EPSPs (fEPSPs) of 0.3–0.5mV in amplitude. A 100Hz tetanus, 1s in duration, x4 with 20s interval (HFS) at 1.5x baseline stimulus intensity was used to induce LTP in the presence of picrotoxin (100μM). The magnitude of the potentiation was calculated at 35–40 min post-tetanus. GluN2B-containing NMDARs and ERK phosphorylation were blocked using Ro25–6981 (1μM) and U0126 (20μM), respectively. Data were collected using an Axopatch-1D or Axopatch 200B amplifier (Molecular Devices, Sunnyvale, CA) at 1000x gain, filtered at 2kHz, and acquired using custom-made software written in Labview (Smith and McMahon, 2005) or pClamp 10 (Molecular Devices, Sunnyvale, CA).

For saturation experiments at TA-CA1, a 20 min baseline was obtained using the same stimulation protocol described for LTP above, followed by 3 consecutive rounds of HFS at 1.5x baseline intensity in the presence of 100μM picrotoxin. The first two HFS rounds were followed by 25 min washout, while the last HFS was followed by a 40 min washout.

AMPAR stimulus response curves were acquired in d,l APV (100μM), as done previously (Smith and McMahon, 2005) and generated by incrementally increasing the stimulus and measuring the fEPSP slope until saturation occurred. The average slope at each stimulus intensity was obtained from 6–10 sweeps/stimulus intensity.

Patch Clamp Recording.

Whole-cell patch clamp recordings were obtained from the soma of CA1 pyramidal cells using the “blind” patch technique (input resistance of 70–180MΩ and a series resistance of 15–25 MΩ with a 10% variance permitted). Borosilicate glass electrodes (5–7 MΩ) were filled with cesium-gluconate pipet solution (in mM): 117 cesium gluconate, 0.6 EGTA, 2.8 NaCl, 5 $MgCl_2$, 2 ATP, 0.3 GTP, 20 HEPES, 5 QX-314 and 0.4% biocytin. A stimulating electrode was placed in stratum radiatum (100–200μm from recorded cell) or placed in stratum lacunosum-moleculare (~450μm from recorded cell) where indicated. The stimulus (0.1Hz, 100μs duration) intensity was set to elicit 100–150pA pharmacologically isolated NMDAR currents by recording at a holding potential of −20 mV and by blocking AMPARs, $GABA_A$Rs, and L-type Ca^{2+} channels using 50μM GYKI 52466, 100μM picrotoxin, and

Author Manuscript Author Manuscript Author Manuscript Author Manuscript

100μM nifedepine, respectively. The GluN2B subunit antagonist Ro25–6981(RO;1μM) was bath applied and the remaining current was subtracted from the NMDAR current to yield GluN2B-containing NMDAR current, as we have done previously (Smith et al., 2010; Vedder et al., 2013). Experiments were collected using an Axopatch-1D amplifier (Molecular Devices, Sunnyvale, CA) at 5x gain, filtered at 2kHz, and acquired in software written in Labview.

Immunohistochemistry and Confocal Microscopy

Recorded cells were filled with biocytin (0.4%). Slices were fixed in 4% paraformaldehyde (PFA) in PBS and stored overnight in PFA. The next day, slices were washed 3x (10min) in PBS and then were incubated in a 10% MeOH and 3.5% H_2O_2 solution in PBS for at least 1h. Following three 10min washes in PBS, slices were exposed to fluorescent streptavidin (lyophilized streptavidin, reconstituted in 1mL PBS and used at 10μL/1mL PBS). Slices were mounted on 3% gelatin coated slides, coverslipped using permafluor (Lab Vision Corp. Fremont, CA), and Z-stacks were acquired using Leica Confocal microscope (100x objective at 2.0 digital zoom, 1.4 n.a.) and Leica Application Suite Software. Spines at proximal and distal dendrites were analyzed if the length from spine head to dendrite was not in excess of 3μm (Harris et al., 1992). Dendritic spines were counted from sections of dendrites 10 μm in length by sequentially moving through individual Z-stacks as we have done previously (Smith et al., 2010; Vedder et al., 2014). The dendritic spines were counted from at least 1–3 segments of dendrite per region in stratum lacunosum-molecular and stratum radiatum from at least 2 recorded cells per rat, from at least 8 rats per vehicle- and E2-treated OVX group using Image J software 1.42q (Wayne Rasband, NIH, USA). Experimenter acquiring images and counting spines was blind to treatment conditions. Spine density is represented as spines/10μm.

Statistical Analysis

Significant differences for the input/output curves and saturating LTP experiments were obtained using two-way ANOVA with repeated measures and Bonferroni post-hoc test and IBM SPSS Statistics 22. Origin 2015 was used to analyze the dendritic spine density using two-way ANOVA with Bonferroni post-hoc, and all other data were analyzed using two sample t-tests. The n number reflects the number of animals. For the spine density and electrophysiology analysis, data from multiple cells or slices from a single rat were averaged to represent the spine density or percent potentiation obtained from that animal. Therefore the n number reflects animal number. Significance was set at $p<0.05$.

Results

E2 Increases Dendritic Spine Density at TA Synapses

We have shown previously that spine density on proximal CA1 dendrites in stratum radiatum (SR) is increased 24 hours (E24) following heightened plasma E2 to proestrous-like levels in ovariectomized (OVX) rats (Smith and McMahon, 2005). From z-stack confocal images of immunostained, biocytin filled CA1 pyramidal cells, we analyzed spine density in stratum lacunosum-moleculare (SLM) where TA synapses are located. In addition, as a positive control, we analyzed dendritic spine density on dendrites in SR in a subset of the same

Author Manuscript Author Manuscript Author Manuscript Author Manuscript

recorded neurons (Fig. 1A and B). We find a main effect of estrogen (Fig.1B; TA: V; 2.93±0.3spines/10μm; n=19 cells/9 animals; E: 3.94±0.3 spines/10μm; 19 cells/9 animals; SC: V; 8.92±0.6 spines/10μm; n=15 cells/9 animals E; 11.19±0.7spines/10μm, n=17 cells/9 animals, two-way ANOVA $F_{(1,31)}$=10.5, p<0.01), as well as a main effect of location ($F_{(1,31)}$=170.3, p<0.001), with no interaction ($F_{(1,31)}$=1.56, p>0.05). Post-hoc means comparison reveals an increase in spine density in SR compared to SLM (p<0.01), as has been previously shown (Megias et al., 2001). These data demonstrate that the effects of E2 on spine density are not specific for dendritic regions where SC-CA1 synapses are located, but also occur in distal regions at the site of TA-CA1 synapses.

E2 Increases AMPAR Transmission and GluN2B-containing NMDAR Current at TA synapses

At SC-CA1 synapses, NMDAR transmission selectively mediated by GluN2B-containing NMDARs is increased without a corresponding increase in AMPAR transmission at E24 (Smith and McMahon, 2006). Therefore, we next investigated the impact of E2 on AMPAR and GluN2B NMDAR transmission at TA-CA1 synapses at this same time point (E24). Unlike at SC-CA1 synapses, AMPAR transmission at TA-CA1 synapses is significantly increased, as shown in the stimulus response curves (Fig. 1C; V: n=7slices/4animals; E: n=7slices/4animals; repeated measures ANOVA, main effect of increasing stimulation $F_{(8,48)}$=84.7, p<0.01; main effect of estrogen treatment $F_{(1,6)}$=8.52, p<0.05 with a significant interaction $F_{(8,48)}$ =6.3 p<0.01). However, similar to our previous finding at SC-CA1 synapses (Smith and McMahon, 2006), pharmacologically isolated GluN2B-containing NMDAR current measured in whole-cell voltage clamp is also significantly increased (Fig. 1D; V: 20±3% GluN2B contribution, n=10cells/8animals; E: 50±8% GluN2B contribution, n=9cells/7animals, two sample t test, p<0.01). These data show that E2 induces a parallel increase in AMPAR transmission and current mediated by GluN2B-containing NMDARs at TA-CA1 synapses at E24, in contrast to our previous findings at SC-CA1 synapses where GluN2B-containing NMDAR current is increased without an increase in AMPA transmission at this same time point (Smith and McMahon, 2005; Smith and McMahon, 2006).

The LTP Magnitude is Not Different at TA-CA1 Synapses in Slices from E2- versus Vehicle-Treated OVX Rats

Given our previous finding that increased GluN2B-containing NMDAR current is causal to the enhanced LTP magnitude at CA3-CA1 synapses at E24 (Smith and McMahon, 2006), we hypothesized that E2 replacement would similarly increase the magnitude of LTP at TA synapses. Alternatively, because AMPAR transmission is also increased at TA-CA1 synapses at E24 unlike at SC-CA1 synapses (which balances the increase in GluN2B-containing NMDAR transmission), the LTP magnitude may not be enhanced at TA-CA1 synapses at E24.

When attempting to induce NMDAR dependent LTP at TA-CA1 synapses, we found it necessary to pharmacologically block $GABA_AR$ inhibition, similar to a previous report (Remondes and Schuman, 2002), likely because strong inhibitory drive during the tetanus prevented effective NMDAR activation (Fig. 2A;without picrotoxin; 104±6% of baseline

Author Manuscript Author Manuscript Author Manuscript Author Manuscript

fEPSP slope; with 100μM picrotoxin; 155±7% of baseline fEPSP slope, one-sample t-test, $p<0.05$). Thus, all LTP experiments were performed in the presence of the $GABA_AR$ blocker picrotoxin.

To investigate differences in LTP magnitude between E2- and vehicle-treated OVX rats, we used 3 rounds of high frequency stimulation (HFS) to induce saturating LTP. This strategy was important to ensure that the experimental conditions used (i.e., inhibition of $GABA_ARs$ and strong HFS) did not mask a potential enhancing effect of E2 on the LTP magnitude. We found that our HFS protocol did not saturate the LTP magnitude with the first round of HFS, as each subsequent round resulted in significant LTP compared to the previous amount of potentiation. Thus, although there was a main effect of LTP stimulation (two way ANOVA with repeated measures; $F_{(2,26)}=16.06$, $p<0.001$, V: n=9 slices/9animals; E: n=6slices/6animals), there were no overall differences in LTP magnitude between E2- and vehicle-treated OVX rats (Fig. 3C; LTP at 3rd tetanus: V:172+11% of baseline fEPSP slope; E2:168+10% of baseline fEPSP slope; no main effect of treatment ($F_{(1,13)}=.385$, $p=0.546$; no significant interaction ($F_{(2,26)}=0.19$, $p=.826$).

E2 Recruits a Role for Synaptic GluN2B-Containing NMDARs and ERK signaling in LTP Induction

In contrast to SC-CA1 synapses, the magnitude of LTP at TA-CA1 synapses is not increased in slices from E2-treated compared to vehicle-treated OVX rats. However, the increase in current carried by GluN2B-containing NMDARs suggests the possibility that LTP induction at TA synapses is dependent upon activation of these NMDARs. In support of this idea, pharmacologically blocking GluN2B-containing NMDARs with the selective antagonist, Ro 25–6981 (RO, 1μM) significantly decreased the magnitude of LTP in interleaved experiments in slices from E2-treated OVX rats (Fig. 3A1; E: 151±12% of baseline fEPSP slope; n=10slices/8animals; E+RO: 128±5% of baseline fEPSP slope; n=9slices/8animals; two sample t test, $p<0.05$).

Next, because ERK activation specifically occurs downstream of synaptic GluN2B-containing NMDAR activation (Krapivinsky et al., 2003; Mulholland et al., 2008), we asked whether blocking ERK activation also participates in LTP induction in E2-treated OVX rats. As predicted, in interleaved experiments, we find that blocking ERK activation using the MEK inhibitor U0126 (20μM) significantly decreased the magnitude of LTP in slices from E2-treated OVX rats (Fig. 3A2; E: 144±7% of baseline fEPSP slope, n=10slices/7animals; E+U0126: 118±2% of baseline fEPSP slope, n=7slices/7animals; two sample t test, $p<0.05$). Because of the reliance of the E2-induced increase in LTP at SC-CA1 synapses on the increase in GluN2B-containing NMDAR current (Smith and McMahon, 2006), we next asked whether the E2-enhanced LTP magnitude at SC-CA1 synapses also requires ERK activation. Unfortunately this was not possible to determine, as blocking MEK caused a significant decrease in the LTP magnitude in vehicle-treated OVX rats (data not shown), in contrast to our findings at TA-CA1 synapses, but consistent with other literature (Sweatt, 2004). Finally, in control experiments in vehicle-treated OVX rats, neither the GluN2B antagonist RO nor the MEK inhibitor U0126 significantly altered the LTP magnitude (Fig. 3B1; V: 150±7% of baseline fEPSP slope; V+RO; 148±7% of baseline fEPSP slope;

Author Manuscript Author Manuscript Author Manuscript Author Manuscript

n=9slices/8animals, two sample t test p>0.05; Fig.3B2 V; 146±9% of baseline fEPSP slope; V+U0126; 154±14% of baseline fEPSP slope, 7 slices/7 animals, two sample t test, p>0.05). Together these data show that proestrous-like E2 levels in OVX rats recruits synaptic GluN2B-containing NMDARs and ERK signaling in the induction of LTP at TA-CA1 synapses.

Discussion

The major findings in this study are twofold: First, E2 increases function of TA-CA1 synapses, indicating that the effect of E2 on hippocampus-dependent learning and memory likely includes enhanced function of these synapses. Second, E2 alters the LTP induction mechanism at TA-CA1 synapses to require activation of synaptic GluN2B-containing NMDARs and ERK, molecules that do not appear to participate in LTP induction at these synapses in vehicle-treated OVX rats. These findings are novel and expand our understanding of how E2 modulates the circuit in hippocampus that likely contributes to enhanced learning and memory following periods of elevated circulating E2. Because the TA pathway can gate activity at SC-CA1 synapses (Manns et al., 2007), the increased synaptic strength observed in the stimulus response curves at TA synapses will likely facilitate depolarization and induction of plasticity at SC-CA1 synapses. In addition, because we show that LTP in slices from E2-treated animals is ERK dependent and ERK activation is downstream of activation of synaptic GluN2B-containing NMDARs (Krapivinsky et al., 2003), it is unlikely that extrasynaptic GluN2B-containing receptors are involved (but see (Zamani et al., 2004). Therefore, our data are consistent with the scenario that E2 recruits synaptic GluN2B-containing NMDARs and ERK to participate in LTP induction at TA-CA1 synapses, which is expected to contribute to the memory enhancing effects of E2.

Previous work in our lab shows that RO blocks the E2-induced increase in novel object recognition (NOR) (Vedder et al., 2013). Whether this is due to E2's effects at SC and/or TA cannot be delineated, as intra-CA1 delivery of RO via stereotaxically placed cannulas likely spreads to proximal and distal dendrites, acting at GluN2B-containing NMDARs at both sites. Electrophysiological data (Aksoy-Aksel and Manahan-Vaughan, 2015; Dvorak-Carbone and Schuman, 1999; Otmakhova et al., 2002; Remondes and Schuman, 2002) support an important role of TA synapses in gating CA1 information processing, and it is possible that changing excitability at distal dendrites leads to altered CA1 information flow which could be linked to altered learning (Ferbinteanu et al., 1999; Hunsaker et al., 2007; Kirkby and Higgins, 1998; Remondes and Schuman, 2004; Vago et al., 2007; Vago and Kesner, 2008; Vnek et al., 1995). Therefore, it is possible that a block of enhanced E2-induced NOR is due not only to enhanced GluN2B function at SC but at TA synapses as well.

An important distinction between our current findings at TA-CA1 synapses and our previous work at SC-CA1 synapses is that E2 increases the LTP magnitude at SC-CA1 synapses (Smith and McMahon, 2005; Smith and McMahon, 2006) while it is unchanged at TA-CA1 synapses at this same time point (E24). In addition, during this same time frame, AMPAR transmission is unchanged at SC-CA1 synapses, but it is significantly increased at TA-CA1 synapses, although spine density is similarly increased (~25%) in SR and SLM. Therefore,

Author Manuscript Author Manuscript Author Manuscript Author Manuscript

the increase in NMDAR:AMPAR ratio that occurs at SC-CA1 synapses, does not occur at TA-CA1 synapses because AMPAR and GluN2B-containing NMDAR transmission are simultaneously increased. This is important because the increase in LTP magnitude at SC-CA1 synapses occurs only when the NMDAR:AMPAR ratio (resulting from the selective increase in GluN2B-containing NMDAR current) and spine density are increased, indicating that enhanced LTP is a likely consequence of an increase in density of silent synapses (NMDA-only containing synapses)(Isaac et al., 1995), which are converted to active synapses following an LTP inducing stimulus. This potential mechanism is further supported by previous data demonstrating that the LTP magnitude is not increased at SC-CA1 synapses 72 hours following elevated plasma E2, coincident with a delayed increase in AMPAR transmission that normalizes the NMDAR:AMPAR ratio, even though dendritic spine density remains increased (Smith and McMahon, 2005). Taken together, our current findings at TA-CA1 synapses strengthens the idea that an increase in silent synapses contributes to heightened plasticity at SC-CA1 synapses, and the lack of an increase in LTP at TA-CA1 synapses results from of an increase in AMPA transmission that occurs simultaneous with the increase in transmission mediated by GluN2B-containing NMDARs, rather than a result of a ceiling effect. However, it is important to point out that even though the LTP magnitude is not increased at TA-CA1 synapses by E2, the recruitment of GluN2B-containing NMDARs and ERK is significant due to their documented role in hippocampal learning (Hebert and Dash, 2002; Tang et al., 1999), together with our previous work showing that intra-CA1 delivery of RO blocks the E2-induced enhanced NOR (Vedder et al., 2013).

Whether E2 recruits GluN2B-containing NMDARs at TA synapses by stimulating new synthesis, increasing phosphorylation of pre-existing receptors, or causing translocation of pre-existing receptors from extrasynaptic sites is not known. Biochemical analyses may not have the resolution to determine an increase in GluN2B subunit protein expression and/or subunit phosphorylation, as studies have failed to show a difference in E2-treated animals (Snyder et al., 2011). However, electrophysiological studies confirm an increase in synaptically mediated GluN2B-containing NMDAR current at SC-CA1 synapses (Smith and McMahon, 2006; Snyder et al., 2011) and recent electrophysiology data form our lab suggest an increase in both NMDAR density and subunit phosphorylation (Vedder et al., 2013). In aged animals, E2 appears to cause an increase in synaptic mobilization of GluN2B-containing NMDARs from extrasynaptic regions (Adams et al., 2004), supporting the possibility that this mechanism participates at TA-CA1 synapses, and potentially an increase in subunit phosphorylation as at SC-CA1 synapses(Vedder et al., 2013). In addition to the role of GluN2B-containing NMDARs and ERK signaling, other mechanisms stimulated by E2 could also participate in the modulation of TA-CA1 synapses. These potential mechanisms include a decrease in the afterhyperpolarization, increase intracellular calcium and phospho-Akt, or an increase in synthesis and release of acetylcholine and/or BDNF (Benten et al., 2001; Bi et al., 2000; Daniel and Dohanich, 2001; Kumar and Foster, 2002; Znamensky et al., 2003). Finally, whether E2 is mediating these effects via classical genomic estrogen receptors, such as ERα, or membrane associated receptors is not known and requires future studies.

Because of the vital role entorhinal cortex plays in facilitating hippocampal dependent memory, our findings provide novel insights into the mechanisms by which E2 effects

Author Manuscript Author Manuscript Author Manuscript Author Manuscript

change in the hippocampal circuit. Subsequent work is necessary to further understand the mechanisms by which TA-CA1 synapses contribute to heightened hippocampal dependent learning with E2 replacement.

Acknowledgements:

We thank Shawn Williams and Ed Phillips in the high resolution imaging facility for assistance with confocal microscopy.

Grant Sponsor: NIH NIMH Grant number: MH 82304 to LLM, Evelyn F. McKnight Brain Institute

Literature Cited

Adams MM, Fink SE, Janssen WG, Shah RA, Morrison JH. 2004 Estrogen modulates synaptic N-methyl-D-aspartate receptor subunit distribution in the aged hippocampus. J Comp Neurol 474(3): 419–26. [PubMed: 15174084]

Aksoy-Aksel A, Manahan-Vaughan D. 2015 Synaptic strength at the temporoammonic input to the hippocampal CA1 region in vivo is regulated by NMDA receptors, metabotropic glutamate receptors and voltage-gated calcium channels. Neuroscience.

Benten WP, Stephan C, Lieberherr M, Wunderlich F. 2001 Estradiol signaling via sequestrable surface receptors. Endocrinology 142(4):1669–77. [PubMed: 11250949]

Bi R, Broutman G, Foy MR, Thompson RF, Baudry M. 2000 The tyrosine kinase and mitogen-activated protein kinase pathways mediate multiple effects of estrogen in hippocampus. Proc Natl Acad Sci U S A 97(7):3602–7. [PubMed: 10725383]

Cordoba Montoya DA, Carrer HF. 1997 Estrogen facilitates induction of long term potentiation in the hippocampus of awake rats. Brain Res 778(2):430–8. [PubMed: 9459564]

Daniel JM, Dohanich GP. 2001 Acetylcholine mediates the estrogen-induced increase in nmda receptor binding in ca1 of the hippocampus and the associated improvement in working memory. J Neurosci 21(17):6949–56. [PubMed: 11517282]

Dvorak-Carbone H, Schuman EM. 1999 Long-term depression of temporoammonic-CA1 hippocampal synaptic transmission. J Neurophysiol 81(3):1036–44. [PubMed: 10085331]

Ferbinteanu J, Holsinger RM, McDonald RJ. 1999 Lesions of the medial or lateral perforant path have different effects on hippocampal contributions to place learning and on fear conditioning to context. Behav Brain Res 101(1):65–84. [PubMed: 10342401]

Frick KM, Fernandez SM, Bulinski SC. 2002 Estrogen replacement improves spatial reference memory and increases hippocampal synaptophysin in aged female mice. Neuroscience 115(2):547–58. [PubMed: 12421621]

Gibbs RB. 1999 Estrogen replacement enhances acquisition of a spatial memory task and reduces deficits associated with hippocampal muscarinic receptor inhibition. Horm Behav 36(3):222–33. [PubMed: 10603286]

Gould E, Woolley CS, Frankfurt M, McEwen BS. 1990 Gonadal steroids regulate dendritic spine density in hippocampal pyramidal cells in adulthood. J Neurosci 10(4):1286–91. [PubMed: 2329377]

Gresack JE, Frick KM. 2006 Post-training estrogen enhances spatial and object memory consolidation in female mice. Pharmacol Biochem Behav 84(1):112–9. [PubMed: 16759685]

Hall JA, Cantley TC, Galvin JM, Day BN, Anthony RV. 1992 Influence of ovarian steroids on relaxin-induced uterine growth in ovariectomized gilts. Endocrinology 130(6):3159–66. [PubMed: 1597136]

Harris KM, Jensen FE, Tsao B. 1992 Three-dimensional structure of dendritic spines and synapses in rat hippocampus (CA1) at postnatal day 15 and adult ages: implications for the maturation of synaptic physiology and long-term potentiation. J Neurosci 12(7):2685–705. [PubMed: 1613552]

Hebert AE, Dash PK. 2002 Extracellular signal-regulated kinase activity in the entorhinal cortex is necessary for long-term spatial memory. Learn Mem 9(4):156–66. [PubMed: 12177229]

Author Manuscript Author Manuscript Author Manuscript Author Manuscript

Henderson VW. 2009 Aging, estrogens, and episodic memory in women. Cogn Behav Neurol 22(4): 205–14. [PubMed: 19996872]

Hunsaker MR, Mooy GG, Swift JS, Kesner RP. 2007 Dissociations of the medial and lateral perforant path projections into dorsal DG, CA3, and CA1 for spatial and nonspatial (visual object) information processing. Behav Neurosci 121(4):742–50. [PubMed: 17663599]

Isaac JT, Nicoll RA, Malenka RC. 1995 Evidence for silent synapses: implications for the expression of LTP. Neuron 15(2):427–34. [PubMed: 7646894]

Kirkby DL, Higgins GA. 1998 Characterization of perforant path lesions in rodent models of memory and attention. Eur J Neurosci 10(3):823–38. [PubMed: 9753151]

Krapivinsky G, Krapivinsky L, Manasian Y, Ivanov A, Tyzio R, Pellegrino C, Ben-Ari Y, Clapham DE, Medina I. 2003 The NMDA receptor is coupled to the ERK pathway by a direct interaction between NR2B and RasGRF1. Neuron 40(4):775–84. [PubMed: 14622581]

Kumar A, Foster TC. 2002 17beta-estradiol benzoate decreases the AHP amplitude in CA1 pyramidal neurons. J Neurophysiol 88(2):621–6. [PubMed: 12163515]

Manns JR, Zilli EA, Ong KC, Hasselmo ME, Eichenbaum H. 2007 Hippocampal CA1 spiking during encoding and retrieval: Relation to theta phase. Neurobiol Learn Mem 87(1):9–20. [PubMed: 16839788]

Megias M, Emri Z, Freund TF, Gulyas AI. 2001 Total number and distribution of inhibitory and excitatory synapses on hippocampal CA1 pyramidal cells. Neuroscience 102(3):527–40. [PubMed: 11226691]

Mulholland PJ, Carpenter-Hyland EP, Hearing MC, Becker HC, Woodward JJ, Chandler LJ. 2008 Glutamate transporters regulate extrasynaptic NMDA receptor modulation of Kv2.1 potassium channels. J Neurosci 28(35):8801–9. [PubMed: 18753382]

Otmakhova NA, Otmakhov N, Lisman JE. 2002 Pathway-specific properties of AMPA and NMDA-mediated transmission in CA1 hippocampal pyramidal cells. J Neurosci 22(4):1199–207. [PubMed: 11850447]

Phillips SM, Sherwin BB. 1992 Effects of estrogen on memory function in surgically menopausal women. Psychoneuroendocrinology 17(5):485–95. [PubMed: 1484915]

Rapp PR, Morrison JH, Roberts JA. 2003 Cyclic estrogen replacement improves cognitive function in aged ovariectomized rhesus monkeys. J Neurosci 23(13):5708–14. [PubMed: 12843274]

Remondes M, Schuman EM. 2002 Direct cortical input modulates plasticity and spiking in CA1 pyramidal neurons. Nature 416(6882):736–40. [PubMed: 11961555]

Remondes M, Schuman EM. 2004 Role for a cortical input to hippocampal area CA1 in the consolidation of a long-term memory. Nature 431(7009):699–703. [PubMed: 15470431]

Rocca WA, Grossardt BR, Shuster LT. 2011 Oophorectomy, menopause, estrogen treatment, and cognitive aging: clinical evidence for a window of opportunity. Brain Res 1379:188–98. [PubMed: 20965156]

Smith CC, McMahon LL. 2005 Estrogen-induced increase in the magnitude of long-term potentiation occurs only when the ratio of NMDA transmission to AMPA transmission is increased. J Neurosci 25(34):7780–91. [PubMed: 16120779]

Smith CC, McMahon LL. 2006 Estradiol-induced increase in the magnitude of long-term potentiation is prevented by blocking NR2B-containing receptors. J Neurosci 26(33):8517–22. [PubMed: 16914677]

Smith CC, Vedder LC, Nelson AR, Bredemann TM, McMahon LL. 2010 Duration of estrogen deprivation, not chronological age, prevents estrogen's ability to enhance hippocampal synaptic physiology. Proc Natl Acad Sci U S A 107(45):19543–8. [PubMed: 20974957]

Snyder MA, Cooke BM, Woolley CS. 2011 Estradiol potentiation of NR2B-dependent EPSCs is not due to changes in NR2B protein expression or phosphorylation. Hippocampus 21(4):398–408. [PubMed: 20082293]

Sweatt JD. 2004 Mitogen-activated protein kinases in synaptic plasticity and memory. Curr Opin Neurobiol 14(3):311–7. [PubMed: 15194111]

Tang YP, Shimizu E, Dube GR, Rampon C, Kerchner GA, Zhuo M, Liu G, Tsien JZ. 1999 Genetic enhancement of learning and memory in mice. Nature 401(6748):63–9. [PubMed: 10485705]

Author Manuscript Author Manuscript Author Manuscript Author Manuscript

Vago DR, Bevan A, Kesner RP. 2007 The role of the direct perforant path input to the CA1 subregion of the dorsal hippocampus in memory retention and retrieval. Hippocampus 17(10):977–87. [PubMed: 17604347]

Vago DR, Kesner RP. 2008 Disruption of the direct perforant path input to the CA1 subregion of the dorsal hippocampus interferes with spatial working memory and novelty detection. Behav Brain Res 189(2):273–83. [PubMed: 18313770]

Vedder LC, Bredemann TM, McMahon LL. 2014 Estradiol replacement extends the window of opportunity for hippocampal function. Neurobiol Aging 35(10):2183–92. [PubMed: 24813636]

Vedder LC, Smith CC, Flannigan AE, McMahon LL. 2013 Estradiol-induced increase in novel object recognition requires hippocampal NR2B-containing NMDA receptors. Hippocampus 23(1):108–15. [PubMed: 22965452]

Vnek N, Gleason TC, Kromer LF, Rothblat LA. 1995 Entorhinal-hippocampal connections and object memory in the rat: acquisition versus retention. J Neurosci 15(4):3193–9. [PubMed: 7722656]

Warren SG, Humphreys AG, Juraska JM, Greenough WT. 1995 LTP varies across the estrous cycle: enhanced synaptic plasticity in proestrus rats. Brain Res 703(1–2):26–30. [PubMed: 8719612]

Woolley CS, Gould E, Frankfurt M, McEwen BS. 1990 Naturally occurring fluctuation in dendritic spine density on adult hippocampal pyramidal neurons. J Neurosci 10(12):4035–9. [PubMed: 2269895]

Woolley CS, McEwen BS. 1993 Roles of estradiol and progesterone in regulation of hippocampal dendritic spine density during the estrous cycle in the rat. J Comp Neurol 336(2):293–306. [PubMed: 8245220]

Woolley CS, McEwen BS. 1994 Estradiol regulates hippocampal dendritic spine density via an N-methyl-D-aspartate receptor-dependent mechanism. J Neurosci 14(12):7680–7. [PubMed: 7996203]

Zamani MR, Levy WB, Desmond NL. 2004 Estradiol increases delayed, N-methyl-D-aspartate receptor-mediated excitation in the hippocampal CA1 region. Neuroscience 129(1):243–54. [PubMed: 15489046]

Zec RF, Trivedi MA. 2002 The effects of estrogen replacement therapy on neuropsychological functioning in postmenopausal women with and without dementia: a critical and theoretical review. Neuropsychol Rev 12(2):65–109. [PubMed: 12371603]

Znamensky V, Akama KT, McEwen BS, Milner TA. 2003 Estrogen levels regulate the subcellular distribution of phosphorylated Akt in hippocampal CA1 dendrites. J Neurosci 23(6):2340–7. [PubMed: 12657693]

Author Manuscript Author Manuscript Author Manuscript Author Manuscript

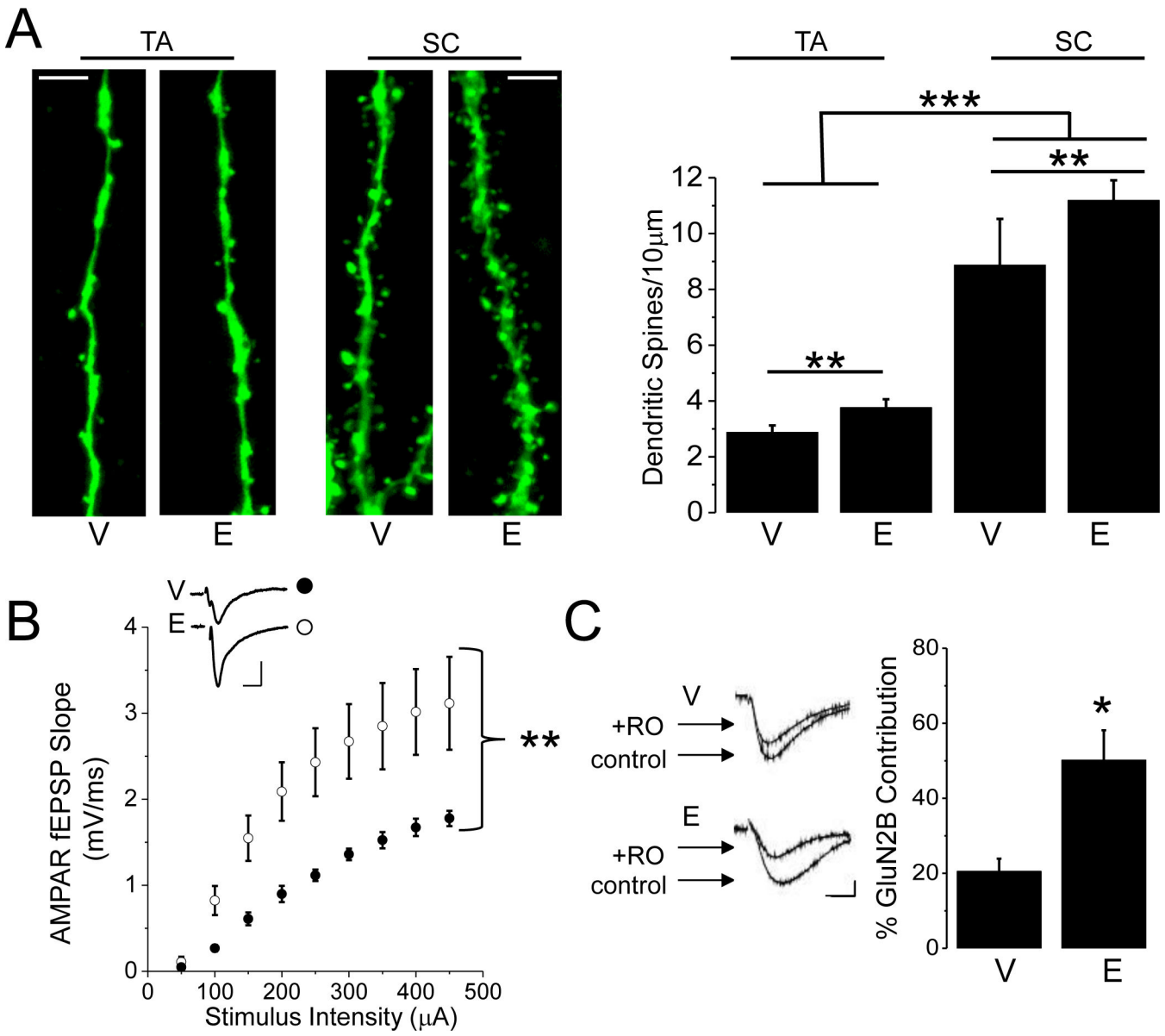

Figure 1:

Proestrous-like E2 increases dendritic spine density, AMPAR transmission, and GluN2B-containing NMDAR current at TA synapses. Representative dendritic segments and bar charts show that E2 replacement increases the density of dendritic spines at TA and SC synapses (TA: V and E, n=19 cells/9 animals; SC: V, n=15 cells/9 animals; E, n=17 cells/9 animals). Scale bars represent 5μm. B, Plot shows stimulus response curves of pharmacologically isolated AMPAR transmission in slices from E2- and vehicle-treated OVX rats (V, n=7slices/4animals; E, n=7slices/4animals). Scale bars represent 0.5mV/10ms. C, Waveforms represent NMDAR current (control) and Ro25–6981 insensitive current (+RO). Bar chart shows E2 increases the % contribution of GluN2B-containing NMDAR current to total NMDAR current (V, n=10cells/8animals; E, n=9cells/7animals). Scale bars: 50pA/20ms. Error bars: SEM. * $p < 0.05$, ** $p<0.01$, *** $p<0.001$.

Author Manuscript Author Manuscript Author Manuscript Author Manuscript

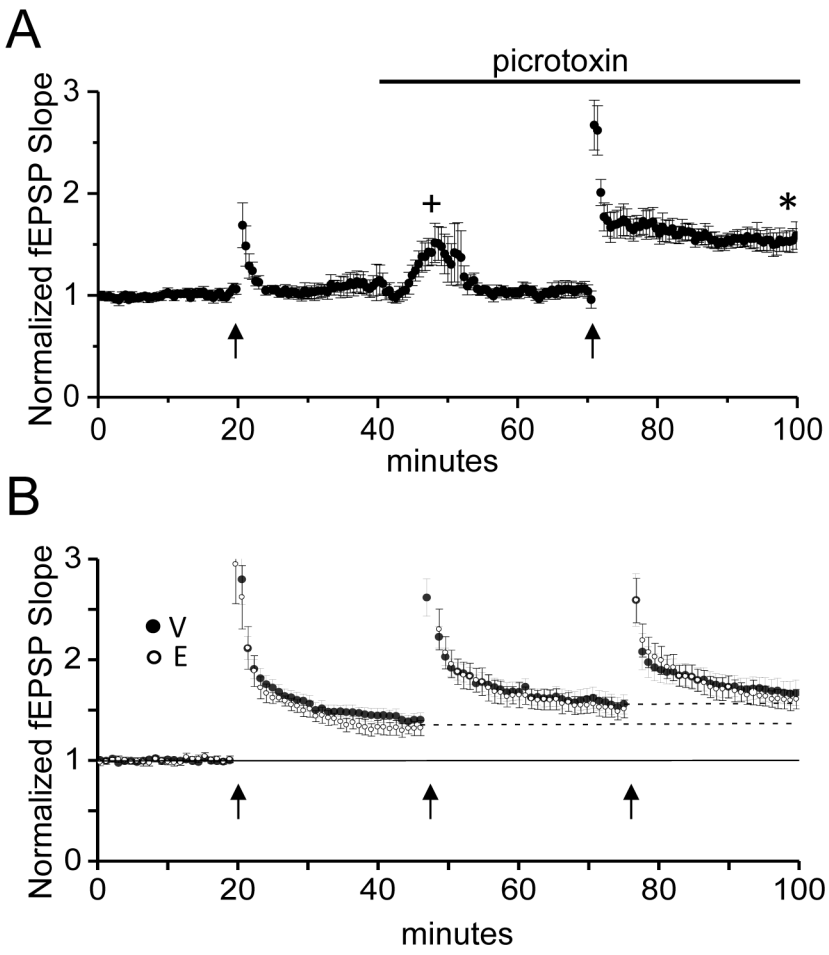

Figure 2:

E2 does not increase the magnitude of LTP at TA synapses. A, Plot shows that blocking $GABA_AR$ with picrotoxin (100μM) is required to induce LTP at TA synapses (n=6 slices/4 vehicle-treated animal). + denotes that the stimulus intensity was decreased to re-establish baseline fEPSP slope. * denotes $p<0.05$. B, Plot shows LTP magnitude induced with 3 rounds of HFS (V: n=9 slices/9animals; E: n=6slices/6animals) is not significantly different between E2- and vehicle-treated groups (two way repeated measures ANOVA, $p>0.05$). Error bars: SEM.

Author Manuscript Author Manuscript Author Manuscript Author Manuscript

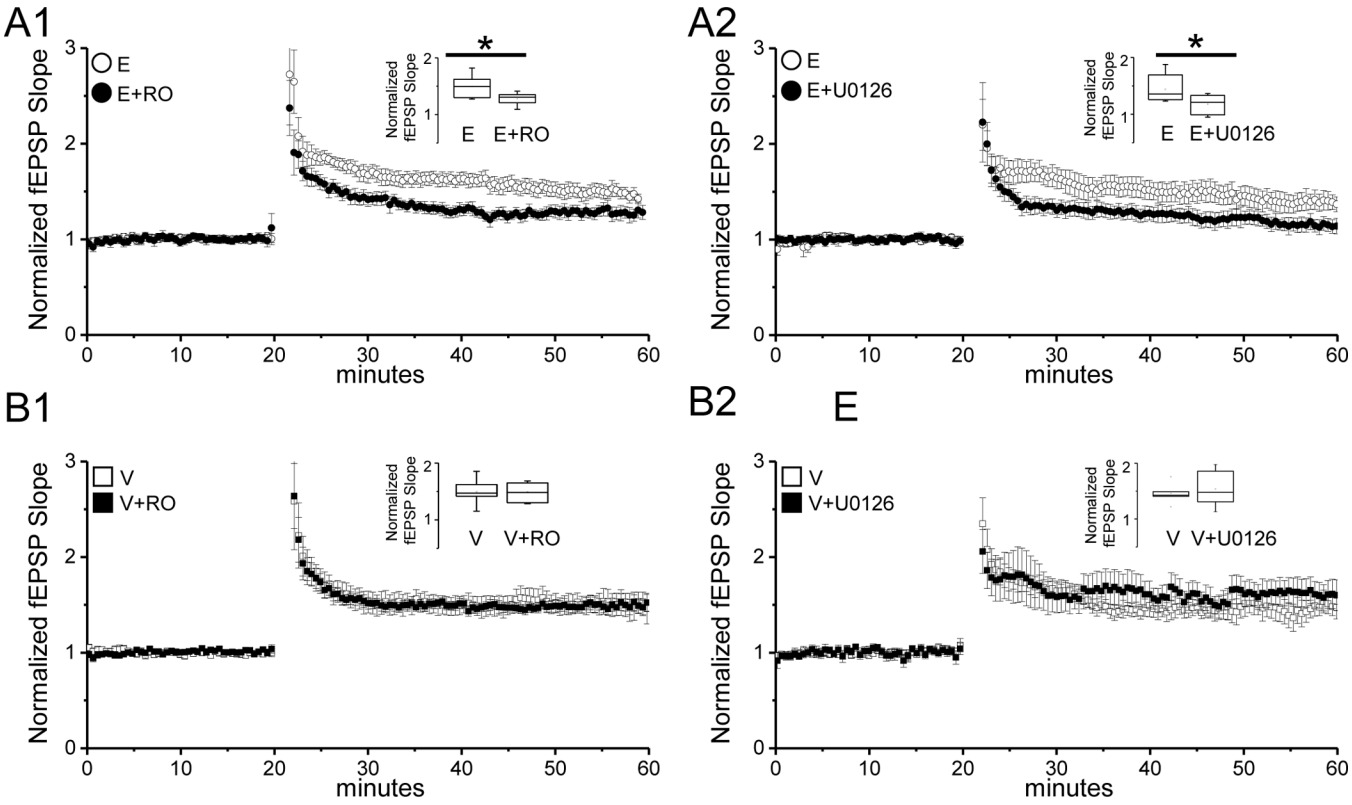

Figure 3:

E2 recruits GluN2B-containing NMDARs and ERK signaling in induction of LTP at TA synapses. A1, A2) Plots show that blocking GluN2B-containing receptors using Ro25–6981 (RO; 1μM) and ERK activation using U0126 (20μM) significantly decreases the LTP magnitude in slices from E2-treated OVX rats (RO: E, n=10slices/8animals; E+RO, n=9slices/8animals; U0126: E, n=10slices/7animals; E+U0126, n=7slices/7animals). B1,B2, Plots show that blocking GluN2B-containing NMDARs using Ro25–6981 (RO; 1μM) or ERK activation using U0126 (20μM) does not alter the LTP magnitude in slices from vehicle-treated OVX rats (RO: V, n=8slices/8animals; V+RO, n=9slices/8animals; U0126: V, n=7slices/7animals; V+U0126; n=7slices/7animals). Insets, box plots show the summarized LTP data for each group. Error bars: SEM. Two sample t test, * denotes $p < 0.05$.